Trends in Computational and Applied Mathematics

Trends in Computational and Applied Mathematics, **25** (2024), e01757
Sociedade Brasileira de Matemática Aplicada e Computacional
Online version ISSN 2676-0029 www.scielo.br/tcam
ORIGINAL ARTICLE
doi: 10.5540/tcam.2024.025.e01757

Enhancing wildfire simulation with wind and vegetation parameters using Cellular Automata in Sete Cidades National Park: a study in the Brazilian Cerrado biome

H. C. BRASIEL[1] and D. A. LIMA[2]

Received on April 18, 2023 / Accepted on July 12, 2024

ABSTRACT. Wildfires pose a significant threat to natural ecosystems, human lives, and properties worldwide. Developing effective prevention and control strategies is crucial for minimizing the risk of catastrophic wildfire events. In this context, computational modelling has emerged as a valuable tool for simulating and analyzing wildfire behavior, which can aid in identifying potential areas for intervention and prevention measures. This article presents a cellular automata model for simulating forest fires in Sete Cidades National Park, Brazil. The model takes into account the wind direction and speed, vegetation type, and probability of burning in a two-dimensional lattice representing the forest area of interest. The simulation output is analyzed to determine the extent of the damage caused by the fire and to identify critical parameters for wildfire propagation. The results highlight the importance of considering wind direction and speed when developing prevention and control strategies for wildfires. By providing insights into the behavior of wildfires, computational modeling can support decision-making processes and facilitate the development of effective policies to manage the risk of wildfires.

Keywords: Forest fires, cellular automata, computational simulation, wildfire propagation, wind direction, prevention measures.

1 INTRODUCTION

Wildfires pose a recurring and severe threat in numerous parts of the world. In Brazil, wildfires are a common method for land preparation for agricultural activities because they are cost-effective [1]. Furthermore, wildfires may occur naturally or be triggered by human actions such as high temperatures, dry weather, electric discharges, spontaneous combustion, low relative humidity, friction between rocks, and even animals' fur rubbing against dry vegetation. However, if caused by humans, they may be considered criminal as they cause significant harm to the flora and fauna of the affected region.

*Corresponding author: Danielli Araújo Lima – E-mail: danielli@iftm.edu.br
[1]Instituto Federal do Triângulo Mineiro (IFTM), Laboratório de Inteligência Computacional, Robótica e Otimização (LICRO), Campus Patrocínio, Minas Gerais, Brazil – https://orcid.org/0000-0002-9792-6154
[2]Instituto Federal do Triângulo Mineiro (IFTM), Laboratório de Inteligência Computacional, Robótica e Otimização (LICRO), Campus Patrocínio, Minas Gerais, Brazil – https://orcid.org/0000-0003-0324-6690

The Cerrado biome, on the other hand, is a resilient ecosystem that has the ability to recover quickly after a fire. The vegetation can regenerate, attracting herbivorous animals looking for new forage, which can feed on insects and reptiles impacted by the fire. Nonetheless, during the dry season, the Cerrado is highly susceptible to wildfires, making modeling the fire propagation in this biome a matter of great importance. It is critical to note that protecting the Cerrado biome [1], which is one of the most biodiverse plant formations, is crucial for the preservation of Brazilian biodiversity and maintenance of the ecosystem services it offers [16]. Therefore, it is imperative to adopt measures to reduce the number of Cerrado wildfires, including raising awareness among the population about the risks and impacts of wildfires, promoting sustainable agricultural practices, and implementing public policies that encourage the biome's conservation [17].

In this regard, the aim of this study is to model wildfire propagation in the Cerrado biome using cellular automata (CA) technique. CA are valuable tools for modeling dynamic systems across various fields, as highlighted by recent research [22]. Mathematicians [19] and computer scientists [2, 6, 13] have extensively studied their applications. In this study, we focus on modeling wildfire propagation in the Cerrado biome, aiming to enhance our understanding of fire behavior in real-world scenarios. Unlike previous works [2, 6, 13] that explored non-real scenarios in the Cerrado biome, our approach involves modeling wildfire propagation in an actual environment to develop more effective fire prevention and control strategies. Utilizing CA offers a detailed perspective on fire propagation patterns, facilitating more accurate predictions regarding the impact of wildfires on the region's flora and fauna. Herein, we considered various types of vegetation, such as homogeneous and heterogeneous vegetation, the fire parameter, and the presence of a river in the middle of the vegetation. We present the results of our experiments and discuss them in the following sections to contribute to the understanding of wildfire propagation in the Cerrado, particularly in the Sete Cidades National Park located in Piauí, Brazil [16, 17]. Our CA model for wildfire propagation in the Cerrado can be an essential tool for environmental planning and management.

2 THEORETICAL FOUNDATION

In this section, we will be discussing the concept of cellular automata and their various applications in different fields. Specifically, we will focus on elementary cellular automata and their applications [23]. We will also explore the popular Game of Life, which is a 2D cellular automaton that is widely used in computer science and other disciplines. Additionally, we will conduct a literature systematic review to investigate the various works related to CA and their applications in different wildfires. Through this review, we hope to gain a deeper understanding of the current state of research in this area and identify potential areas for future research.

2.1 Cellular Automata

A CA is considered a discrete computational and mathematical model consisting of a regular grid of cells, each of which can be in a finite number of states S_i, where (i) is a finite number. The state of each cell evolves over time according to a set of rules that depend on the current state of the cell and its neighboring cells [13]. The update rules are typically simple and local, meaning that they only involve a small number of cells at a time and do not depend on the global state of the system.

2.1.1 Elementary cellular automata

Elementary cellular automata (ECA) are a class of one-dimensional, discrete dynamical systems that exhibit simple and yet complex patterns of behavior. ECA consist of a linear array of cells, each with a binary state (0 or 1) that evolves over time according to a set of local transition rules, considering the radius r that depend only on the current state of the cell x_i and its two nearest neighbors η_i^m, where $(m = 2 \times r + 1)$ [12]. The transition rules can be specified by a lookup table, where each possible configuration of the three-cell neighborhood is associated with a new state for the central cell in the next time step. Despite the simplicity of the rules, ECA can produce a wide variety of patterns ranging from static, repeating patterns to complex, seemingly random behavior. ECA have applications in various fields such as cryptography [14,23], robotics [10,15], artificial life [4] and the study of emergent properties in complex systems [12].

2.1.2 Game of Life

A two-dimensional cellular automaton (2D-CA) is a discrete dynamical system that operates on a grid of cells arranged in a two-dimensional lattice. Each cell can take on a finite number of possible states, and its state changes over time based on the state of its neighboring cells. The update rule for each cell is typically a function of the states of its immediate neighbors, and the rule is applied simultaneously to all cells at each time step. The two-dimensional lattice can be periodic or non-periodic, and the boundary conditions can be set to be either fixed or dynamically updated. The 2D-CA have been used to model a wide variety of physical, biological, and social phenomena, including fluid dynamics and crystal growth [25], traffic flow [24] and forest fires [2,6,13].

The Game of Life is a well-known 2D-CA that consists of a grid of cells that can be in one of two states, alive or dead, created by J. Conway (1970) [13]. The state of each cell depends on the states of its neighbors η_{ij}^m, where $m = (2 \times r)^3 + 1$ in a given generation, and the rules for transitioning from one generation to the next are simple: a dead cell with exactly three living neighbors becomes alive, a living cell with two or three living neighbors remains alive, and a living cell with fewer than two or more than three living neighbors dies [13]. These simple rules can lead to complex and interesting patterns of behavior, including oscillators, gliders and spaceships. The Game of Life is an example of emergent behavior [6], where the overall behavior of the system arises from the interactions of its individual components.

2.2 Related works

Wildfire propagation is a critical issue in environmental protection and disaster management. The use of cellular automata (CA) models for simulating wildfire propagation has been researched widely in recent decades. Various studies have shown the effectiveness of CA models in modeling the spread of wildfires, as it is possible to see in Table 1.

In order to carry out a more precise search on wildfire modeling works through CA, we carried out a Systematic Literature Review (SLR) through the Scopus platform and Google Scholar, based on the work of [11]. The tool to conduct the SLR was carried out in the Software StArt[1] (State of Art) [5]. The protocol, inclusion (IC) and exclusion (EC) criteria were defined. The inclusion criteria established in the protocol are: (IC.1) be an article written in English, (IC.2) be a primary article, (IC.3) be an article written between 2017-2022 and (IC.4) be a modeled article within a specific real scenario. Exclusion criteria included (EC.1) not being an article in English, (EC.2) being a short article, (EC.3) not being a peer-reviewed article, (EC.4) being an article written before 2017. Done this, and articles were identified to the research question: "What are the articles that use cellular automata to carry out fire modeling in specific forests?".

Thus, 50 works were found that met the initial criteria through the following search string: "(cellular `AND` (automata `OR` automaton) `AND` (fire `OR` spread `OR` wildfire) `AND` (forest `OR` biome))". Figure 1a represents a word cloud that represents the initial identification of the works found. From the word cloud it is possible to see that the most recurrent words were: "cellular automata", "deforestation" and "fires". After this initial step, the articles were read and selected. In this first stage, we selected 20 articles from the initial reading of the TAK (title, abstract and keywords) of each article. However, in the final part we read the 20 complete articles and thus extracted for this study only 6 articles, see Table 1, and will be explained below.

Table 1: Selected articles from the last 5 years of research on CA in wildfire modeling considering: Start paper ID, title, authors, publication year, priority reading level, Start score.

ID	Title	Authors	Year	Level	Score
1	Automatic evolutionary adjustment of a cellular automata model for forest fire propagation	[6] Ferreira; Quinta; Lima; Martins & Oliveira	2022	Very high	74
5	Dynamic simulation of fire propagation in forests and rangelands using a GIS-based cellular automata model	[7] Gharakhanlou & Hooshangi	2021	Very high	90
8	Research on Amazon Forest Fire Based on Cellular Automata Simulation	[21] Sun; Wei; Chen & Ren	2021	Very high	77
10	Identification before-after forest fire and prediction of mangrove forest based on Markov-cellular automata in part of Sembilang national park, Banyuasin, south Sumatra, Indonesia	[3] Darmawan; Sari; Wikantika; Tridawati; Hernawati & Sedu	2020	Very high	84
13	Intelligent management occurrence and spread of front fire in GIS by using cellular automata case study: Golestan forest	[9] Hesam & Valizadeh	2019	Very high	76
15	Cellular automata simulation of forest fire behavior on Italian landscape: The case of Sardinia	[8] Giannino; Russo; Ascoli; Migliozzi; Siettos & Mazzoleni	2017	Very high	51

[1] State of Art (StArt) developed in LaPES - Laboratório de Pesquisa em Engenharia de Software, Federal University of São Carlos (UFSCar). Link: `http://lapes.dc.ufscar.br/tools/`.

Fire propagation modeling is a critical issue to prevent and control the damage of forest fires, which have faced a significant increase due to climate change threatening different biomes [6]. Tuning the various parameters involved in these models is a challenging task, and a method of parameters adjustment of fire propagation models based on genetic algorithms was proposed. Different experiments in various scenarios showed that it was possible to use evolutionary computation that automatically adjusts the parameters of a fire spread model [6]. According to [7] wildfire propagation modeling has become a critical issue in environmental protection and disaster management. The authors proposed a Geographic Information System (GIS)-based cellular automata (CA) model in their work [7], which accounts for wind speed and direction, vegetation density, and topographic conditions as influential factors in wildfire propagation. They used a genetic algorithm (GA) to calibrate the model, and validation using an independent fire case showed that the proposed model could effectively simulate wildfire propagation. The study concludes that the model's results can assist fire managers in predicting fire propagation to better control wildfires.

Another study [21] crafted a hierarchical clustering model for simulating Amazon forest fire spread via cellular automata. It optimized wildfire risk index ranking through entropy weight TOPSIS (Technique for Order Preference by Similarity to Ideal Solution) and validated the method's viability through simulations. Conversely, [3] applied an integrated Markov Chain and CA model to anticipate mangrove forest changes in Indonesia's Sembilang National Park. The study examined "pre" and "post-1997" forest fire conditions in Indonesia, the country's most severe forest fire incident, employing remote sensing via Landsat satellite imagery. It revealed periodic changes in the mangrove ecosystem attributable to effective government management.

In a study conducted in the Golestan region's jungles, the CA model was based on layers such as height, slope, aspect, vegetation density, roads, rivers, and climate, with a general accuracy of 65% and Cohen's kappa coefficient of 59% [9]. A CA modeling framework was used to simulate the evolution of two small-size wildland fires that broke out in Sardinia, Italy, in 2010 [8]. Although simulation results over an ensemble of lattice realizations showed that the model captures the actual data qualitatively, significant quantitative differences between simulations and real patterns exist for very small sizes of burned area [8].

After reading works, CA-models have been used effectively to model the spread of wildfires in different part of the world in last 5 years, as is possible to see in Figure 1b. The world map showing the location of natural parks modeled by CA as found by SLR. The colors in red represent the country that used CA the most for modeling forest fires, in this case Brazil with two works, one for the Amazon Forest and the other for Savannah, while the other countries: Canada, Indonesia, Iran and Italy (in green) had occurrence of one article published for the modeling of fires and fires with CA. After conducting the SLR, it was observed that the authors considered various factors, including landscape characteristics, flammability, wind patterns, and climate.

In contrast to precursor models such as those proposed by Ferreira et al. [6] and Gharakhanlou et al. [7], our paper introduces several advancements in wildfire propagation modeling. While previous studies focused on homogeneous vegetation [13] or a limited number of heterogeneous

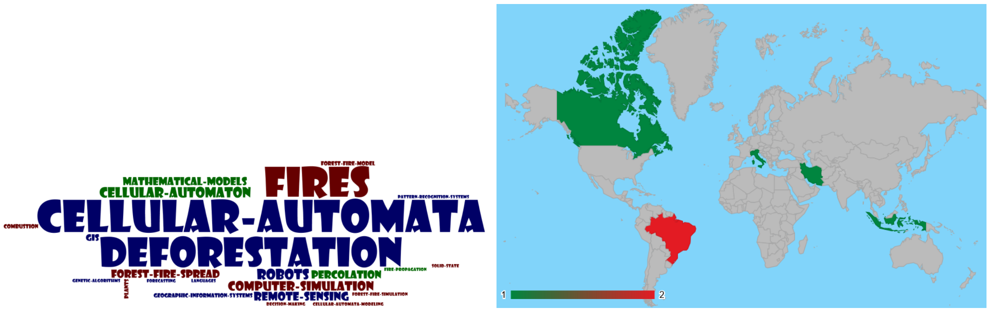

(a) Word cloud. (b) World map.

Figure 1: Word cloud and world map resulted from the initial SLR methodology.

states [2], our model incorporates five distinct vegetation states to better capture the complexity of real-world scenarios. Additionally, while some precursor models considered factors like rivers [2], our model omits this consideration to streamline the simulation process. Notably, unlike Ferreira et al. [6], who employed Genetic Algorithms for parameter adjustment, we do not utilize this method in our approach. Furthermore, to enable the practical application of our model to real-world scenarios in Sete Cidades National Park, we implemented a clustering approach to transform real images into clustered images capable of being reproduced by cellular automata. These enhancements contribute to a more comprehensive and accurate representation of wildfire spread dynamics, ultimately aiding in the development of effective strategies for fire prevention and control in the Cerrado biome.

2.3 Context for the proposed model

The cellular automaton model used in our work is a two-dimensional lattice with non-periodic boundary conditions, where each cell in the lattice represents a small portion of the forest. The dimension of the lattice is set according to the area of interest. Each cell in the lattice can be in one of 12 possible states, including five vegetation states representing the type of vegetation in the forest, and six burning states representing the intensity of the fire, and one state representing the dead forest. The vegetation is assumed to be homogeneous in the forest, and each cell has the same probability of burning as its neighbors, depending on the vegetation type. The update rule used in the model is a probabilistic rule, where the state of each cell is updated at each time step based on its current state and that of its neighboring cells. The update rule type is asynchronous, which means that the state of each cell is updated in a random order at each time step. The update rule also takes into account the wind parameter, which is modeled by a matrix of wind preferences. The time step used in the model is set to $t_{b_i} = 1 \in S_B$ and the CA evolves over T time steps, in this case, we considered $T = 100$ or until all lattice cells are in the dead (black) state.

3 PROPOSAL

In this section, we will present our proposed model that incorporates three key parameters: fire control, wind modeling using the preference matrix, and vegetation modeling in the Sete Cidades National Park. We will conduct experiments and take into account the fire control strategy to simulate the fire propagation accurately. Next, we will discuss the modeling of wind and how it influences the spread of wildfires. Then, we will explore into the vegetation modeling and its impact on the behavior of wildfires in the Brazilian Cerrado biome. Finally, we will present the general algorithm that integrates these three parameters to simulate wildfire behavior and propagation accurately.

3.1 Fire spread

To simulate fire spread, we employ a CA model where each cell can exist in one of three main states: $S = \{s_A, s_B, s_D\}$, and 12 possible sub-states. Here, $s_A \in \{s_{A_{RF}}, s_{A_{EF}}, s_{A_{SC}}, s_{A_{TC}}, s_{A_{RC}}\}$ (alive states, each representing a type of Cerrado vegetation found in Sete Cidades National Park, which will be detailed in Section 3.3), s_D (dead state) and $s_B \in \{s_{B_{y_1}}, s_{B_{y_2}}, s_{B_{o_1}}, s_{B_{o_2}}, s_{B_{r_1}}, s_{B_{r_2}}\}$ (burning states), that change over time, as is possible to see in Figure 2. A green cell indicates an intact forest s_A while yellow $s_{B_{y_1}}$ and dark yellow $s_{B_{y_2}}$ cells represent a fire that has just started (Figures 2a and 2b). The orange cells, both light $s_{B_{o_1}}$ and dark $s_{B_{o_2}}$ (Figures 2c and 2d), represent intermediate stages of burning, while the red cells, also light $s_{B_{r_1}}$ and dark $s_{B_{r_2}}$ (Figures 2e and 2f), represent a fire that has been burning for a long time. Finally, black cells s_D indicate that the forest's cell has died (Figures 2g). Each cell that is burning has a probability of $p(x_{ij}) \neq 0$ of spreading the fire to neighboring cells [20]. We assume that the vegetation is homogeneous in the forest, meaning that each cell has the same probability of burning as its neighbors. The time that each cell stays in a fire color is set to $t_{b_i} = 1$, and at each time step, the model updates the state of each cell based on its current state and that of its neighbors. By simulating the spread of fire using this CA model, we can predict how the fire will spread over time and help prevent the damage caused by wildfires.

3.2 Wind direction

The wind is an important parameter that affects the spread of fire in different directions. Additionally, modeling wind direction and velocity is crucial in a CA wildfire model as it allows for a more accurate representation of fire spread, taking into account the potential changes in direction and speed that can significantly affect the fire's behavior. Herein wind is modeled by a $W_{3\times3}$ matrix of wind preferences [18], where the center cell represents the current position of the fire and the eight surrounding cells represent the direction of the wind. The matrix of preferences of our work is based on Lima & Lima [13] and Schadschneider et al. [18].

In our model, the wind parameter $\vec{w}$ has values ranging from 0 to 20, where 0 represents no wind (Figure 3a), 2 represents a light wind (Figure 3b), 10 represents intermediate wind (Figure 3c) and 20 represents very strong wind (Figure 3d). As the wind speed increases, the fire is more

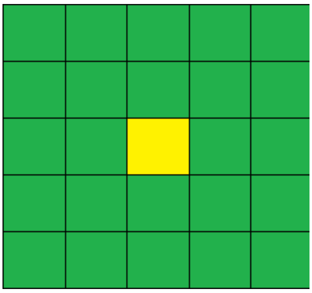

(a) $t = 0$.

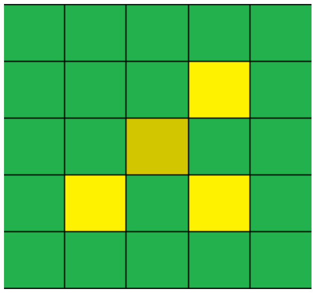

(b) $t = 1$.

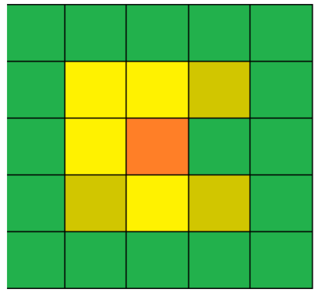

(c) $t = 2$.

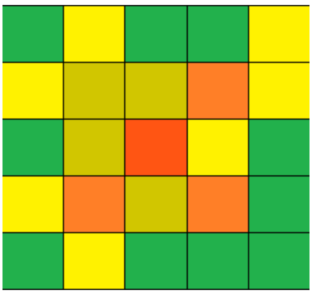

(d) $t = 3$.

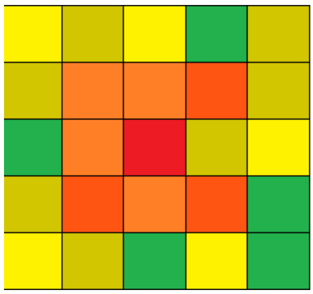

(e) $t = 4$.

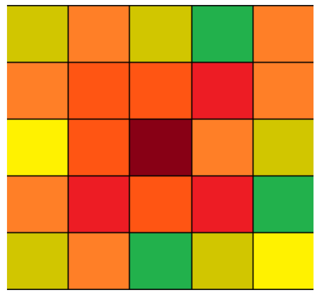

(f) $t = 5$.

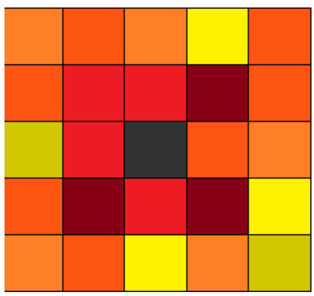

(g) $t = 6$.

Figure 2: Transitions of the CA to states between cells: (T_A) alive (green), (T_{B_i}) burning (yellow, yellow, orange and red) and (T_D) dead (black).

likely to spread in the direction of the wind. Figure 3 shows the effect of wind on the spread of fire, where four different wind preference matrices are used, each with a different wind parameter value. It can be observed that the higher the wind parameter value, the more the fire spreads in the direction of the wind, in this case, the wind direction is west-east (left-right).

3.3 Vegetation modeling

In our proposal, different types of vegetation have varying levels of flammability, which can significantly impact the spread and intensity of a wildfire. By incorporating different types of vegetation in a CA wildfire model, we can better predict the behavior of a fire in a specific area

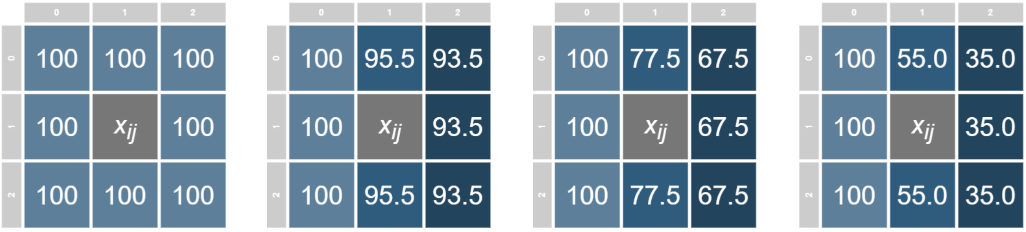

(a) $\vec{w} = 0$. (b) $\vec{w} = 2$. (c) $\vec{w} = 10$. (d) $\vec{w} = 20$.

Figure 3: Fire spread was considered using a wind preference matrix inspired by the works of Schadschneider [18] and Lima & Lima [13].

and develop more effective prevention and control strategies. Figure 4 shows the steps taken to transform the map vegetation of the Sete Cidades National Park maps [16, 17] into a 2D-CA L lattice. This involves scanning the real map and dividing it into pixels, each of which represents a single cell in the digital grid. The L cells are created by considering the neighborhood of each pixel and assigning it to one different vegetation state S_A (alive forest). The size of the pixels can be adjusted to match the desired resolution of the digital grid, and the resulting L grid can then be used as the basis for the CA wildfire model. Than we replace the probability of each cell x_{ij} burn depending on the vegetation type. The vegetation burning probabilities are considered for five types of vegetation, based on Matos' work [16] and Oliveira's work [17].

The riparian forest ($s_{A_{RF}}$) is the most humid vegetation and has a lower probability of burning (10%). Evergreen forest ($s_{A_{EF}}$) has a probability of burning $p(x_{ij})$ of 25%. Savannah Cerrado (Cerradão), state ($s_{A_{SC}}$), has a higher probability of burning (45%), followed by Typical Cerrado (65%), state ($s_{A_{TC}}$), and Rupestrian Cerrado (80%), state ($s_{A_{RC}}$). These probabilities are used to calculate the probability of each cell burning in the cellular automaton model. The transformation process shown in Figure 4 includes the selection of the vegetation types present in the Sete Cidades National Park and their respective probabilities of burning. The result is a map of the area with different vegetation types and probabilities of burning $\forall x_{ij} \in L$.

3.4 Algorithm overview

Forest fires can cause significant damage to natural habitats, leading to loss of life, property, and biodiversity. To prevent such disasters, it is important to understand how fires spread and develop mitigation strategies accordingly. A cellular automaton model is one approach for simulating fire spread that can provide insights into the behavior of fires in different conditions. In this algorithm, we present a step-by-step approach for simulating forest fire spread using a cellular automaton model. The algorithm includes initializing the model with a lattice representing the forest area of interest, assigning each cell a state corresponding to its vegetation type and probability of burning, setting the wind preference matrix, and updating the state of each cell for each time step based on specific rules.

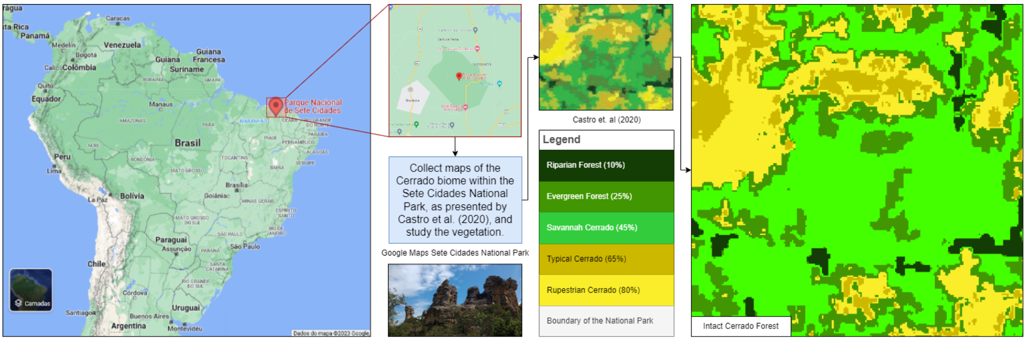

Figure 4: Steps for carrying out the transformation of the vegetation of the Sete Cidades National Park into a two-dimensional celullar automaton lattice.

1. Initialize the model with a two-dimensional $L_{200\times200}$ lattice representing the forest area of interest, in this case Sete Cidades National Park.

2. Assign each cell $\forall x_{ij} \in L$ a state corresponding to its vegetation type and probability of burning based on transformation process shown in Figure 4.

   (a) Riparian forest ($s_{A_{RF}}$) is the most humid vegetation and has a lower probability of burning (10%).

   (b) Evergreen forest ($s_{A_{EF}}$) has a probability of burning $p(x_{ij})$ of 25%, which represents denser vegetation.

   (c) Savannah Cerrado (Cerradão), state ($s_{A_{SC}}$), has a higher probability of burning (45%), followed by Typical Cerrado (65%), state ($s_{A_{TC}}$), and Rupestrian Cerrado (80%), state state ($s_{A_{RC}}$).

3. Set the time that each cell stays in a fire color (buring state) to $t_{b_i} = 1 \in T$, that means at each time step t fire color changes.

4. Set the wind preference matrix $\vec{w}$ according to the wind direction and speed, where 0 represents no wind and 20 represents very strong wind.

5. For each time step, iterate over each cell in the lattice and update its state based on the following rules:

   (a) If the cell is in a fire state (yellow $s_{B_{y_1}}$, dark yellow $s_{B_{y_2}}$, orange $s_{B_{o_1}}$, dark orange $s_{B_{o_2}}$, light red , $s_{B_{r_1}}$ or dark red $s_{B_{r_2}}$), it will remain in that state for the next time step with a probability of 1.

   (b) If the cell is in an intact state (green), it will transition to a fire state with a probability of $p(x_{ij})$ if one or more of its neighboring cells is in a fire state.

(c) If the cell is in a fire state and is adjacent to a cell in an intact state, it will ignite that cell with a probability of $p(x_{ij})$.

(d) If the cell is in a fire state and is adjacent to a cell in a fire state, the fire will spread from the cell with the highest wind preference in the direction of the wind with a probability of $p(x_{ij})$.

6. Repeat step 5 until the fire has burned out or the simulation has reached a predetermined number of time steps.

7. Analyze the output of the simulation to determine the extent of the damage caused by the fire and to identify potential areas for intervention and prevention measures.

This algorithm do not assumes that vegetation is homogeneous, meaning that all cells $x_{ij} \in L_{200\times200}$ have different probability of catching fire depending on vegetation type. If there are other different types of vegetation in Sete Cidades National Park, with different flammability characteristics [2, 16, 17, 20], the probability of spreading the fire may need to be adjusted accordingly. The output of the simulation can help identify potential areas for intervention and prevention measures to minimize the damage caused by forest fires.

4 RESULTS

The experiments carried out here aim to carry out qualitative comparisons about the effect of changing some of the parameters of the fire propagation model in homogeneous forests, considering 2D-CA with $L_{200\times200}$ cells, with probabilistic transition rules and non-periodic contour. The probability of fire varies significantly among the different types of vegetation found in Sete Cidades National Park. The probabilities of fire occurrence for each type of vegetation are clearly presented in Figure 4. The simulation starts with a cell on fire and the fire spread is updated for each cell at each time t step (iteration). The result of the simulation is a visual representation of fire spread, which can be used to analyze different scenarios and understand how fire spread is affected by different factors and variables. Besides that it is possible to calculate B_F that means percentage of forest burned by wildfire. In the experiments carried out, the effect of varying the wind parameter on the propagation of fires in heterogeneous forests was compared. The simulation was conducted with the wind ($\vec{w}$) parameter varying from 0 (no wind) to 20 (extremely strong wind). The effect of wind over time was also analyzed, and for this purpose the simulations in $T = \{20, 40, 60, 80\}$ were taken.

4.1 Simulations without parameter wind

The first experiment Figure 5, the wind parameter was set to zero ($\vec{w} = 0$) and it was observed that the fire spread evenly in all directions. This suggests that without the wind effect, it is possible to observe that the wind propagates in a circular and proportional way from the center to the edges of the lattice, considering $T = \{20, 40, 60, 80\}$. By keeping the wind parameter at zero, it is possible to isolate the effect of wind on fire spread and observe how other factors, such as vegetation, contribute to the spread of wildfire. In Figure 5a in $t = 20$ it is possible to observe that fire spread in a circle way and only two types of vegetation was affected, Savannah Cerrado (Cerradão) and Evergreen Forest, but the probability of burn is different for each one and percentage of burned forest is $B_F = 2.25\%$. In Figure 5b in $t = 40$ it is possible to observe that fire is advanced and the forest burned $B_F = 8.87\%$. In Figure 5c, $B_F = 22.86\%$ whereas Figure 5d, $B_F = 42.84\%$ and all type of vegetation was burned by wildfire. This finding highlights the importance of considering wind in wildfire management and prevention strategies.

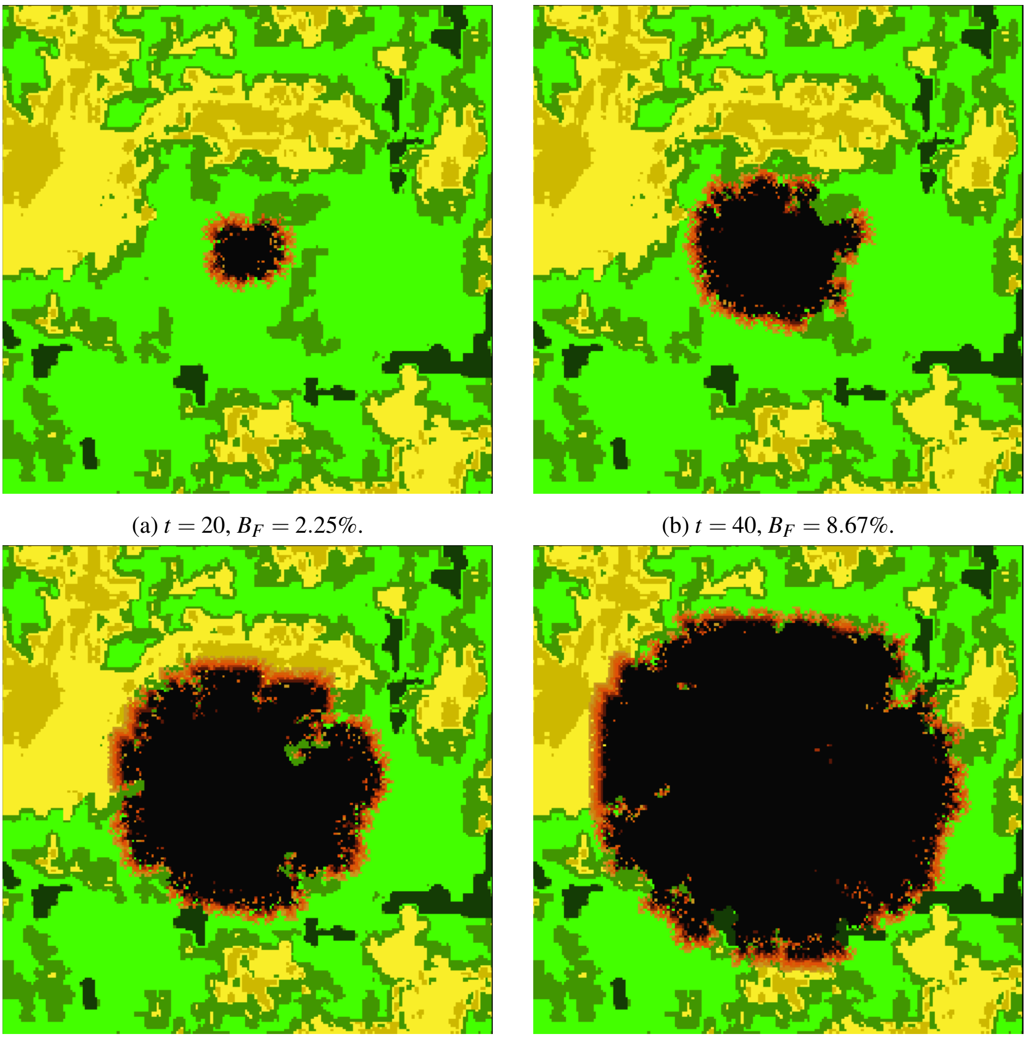

(a) $t = 20$, $B_F = 2.25\%$.

(b) $t = 40$, $B_F = 8.67\%$.

(c) $t = 60$, $B_F = 22.86\%$.

(d) $t = 80$, $B_F = 42.84\%$.

Figure 5: Experiments without considering wind $\vec{w} = 0$ spread.

4.2 Simulations considering wind direction west-east

The wind parameter was increased to $\vec{w} = 5$, and the simulation showed that the fire spread started to tend towards the right. The fire spread faster towards the wind direction, with the cells burning more often and more intensely. The variable B_F indicates the proportion of burned forest after (t) CA-steps. Figure 6 shows the results of the experiment with the wind direction set to west-east.

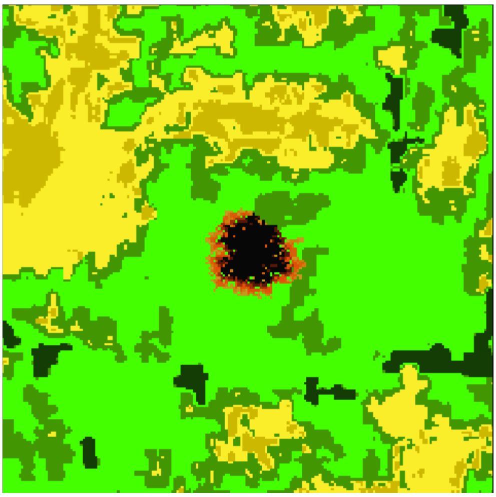

(a) $t = 20$, $B_F = 2.38\%$.

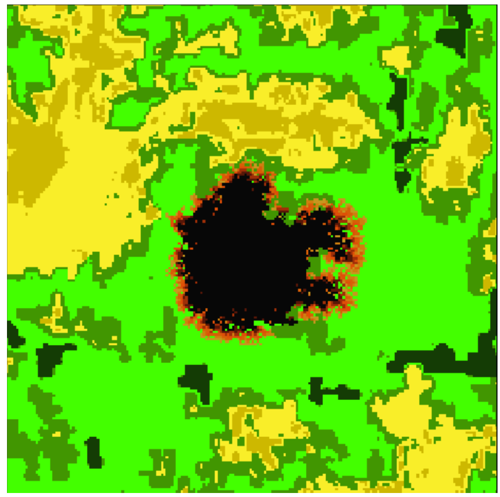

(b) $t = 40$, $B_F = 9.68\%$.

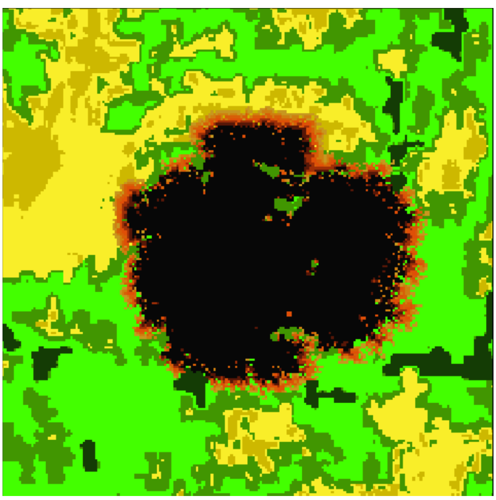

(c) $t = 60$, $B_F = 25.95\%$.

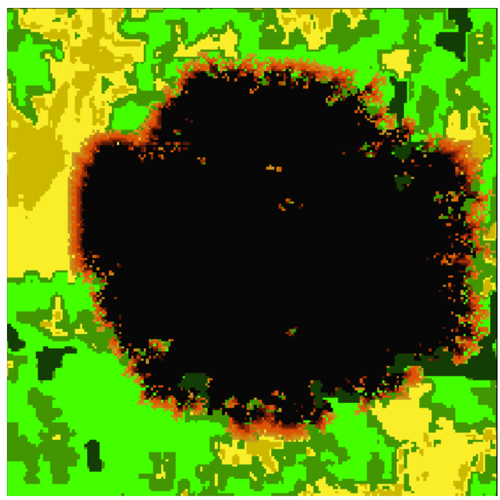

(d) $t = 80$, $B_F = 48.68\%$.

Figure 6: Experiments considering wind $\vec{w} = 5$ direction west-east.

As time passed, the burned forest proportion increased considerably, with 2.38% at $t = 20$ (see Figure 6a), 9.68% at $t = 40$ (see Figure 6b), 25.95% at $t = 60$ (see Figure 6c), and 48.68% at $t = 80$ (see Figure 6d).

The wind parameter was increased to $\vec{w} = 10$, and the simulation showed that the fire spread became even more intense downwind, see Figure 7.

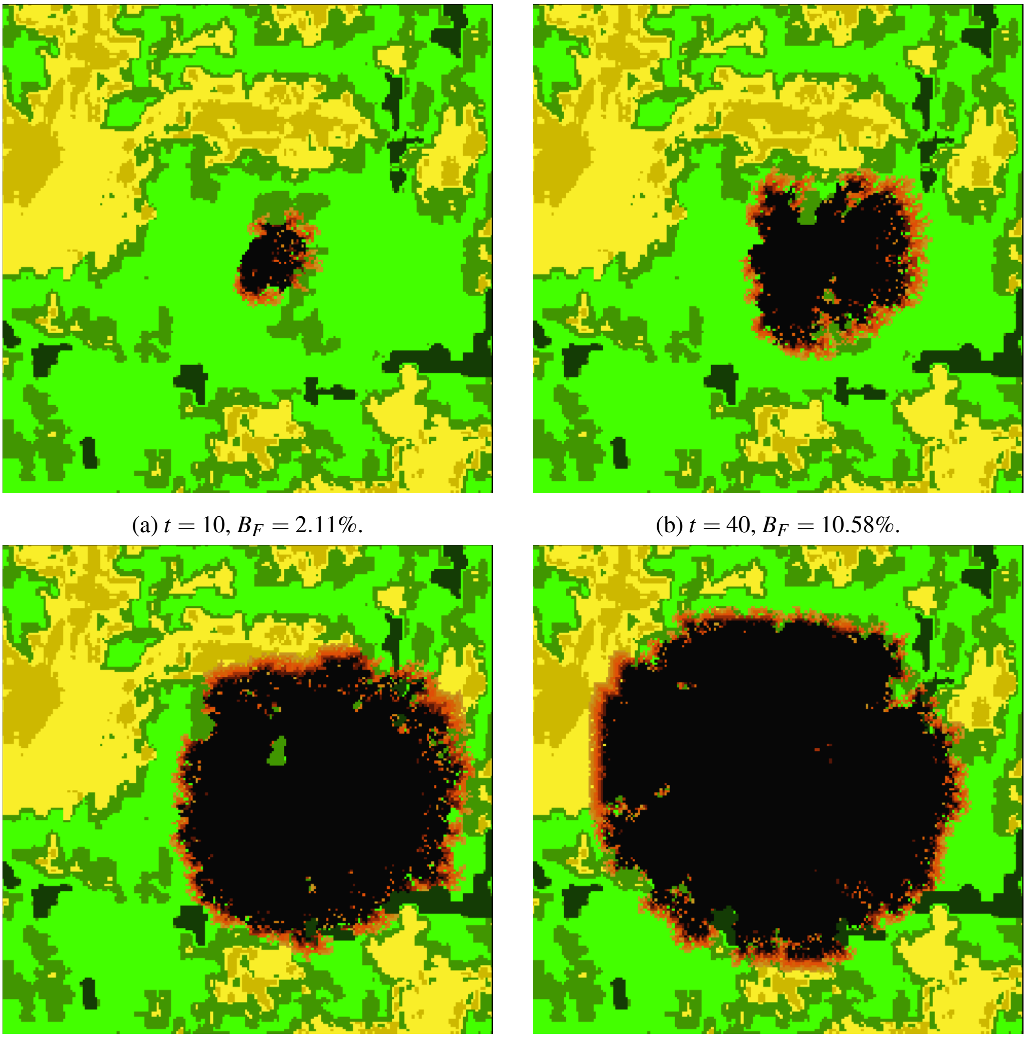

(a) $t = 10$, $B_F = 2.11\%$.

(b) $t = 40$, $B_F = 10.58\%$.

(c) $t = 60$, $B_F = 28.74\%$.

(d) $t = 80$, $B_F = 48.02\%$.

Figure 7: Experiments considering wind $\vec{w} = 10$ direction west-east.

The Figure 7a shows the fire propagation at $t = 10$ with a fire spread rate of $B_F = 2.11\%$. At this stage, the fire is still incipient, and only a few cells have been burned. However, the wind is already having an impact on the fire spread, with the fire advancing more aggressively towards the east, where the wind is blowing. As time progresses, the fire spreads more rapidly in the direction of the wind, as shown in Figure 7b, where $t = 40$ and $B_F = 10.58\%$. The fire front has already covered a considerable distance, with a significant number of cells being burned in the eastern part of the simulation area. The western side of the area has been less affected, with a lower rate of burning. Figure 7c displays the fire spread rate at $t = 60$, where $B_F = 28.74\%$. At this point, the fire has already covered a large portion of the environment, with a particularly intense fire front in the eastern part of the region. The rate of burning has increased significantly compared to the previous figure, with cells burning more frequently and intensely. Finally, Figure 7d presents the simulation's results at $t = 80$, where the wind parameter was set to zero. In this case, the fire front has spread predominantly towards the east, where the wind was blowing earlier in the simulation. The final burn rate is $B_F = 48.02\%$, which indicates that almost half of the environment has been burned. Cells burned with greater frequency and intensity towards the wind, while cells on the opposite side had a lower burning rate.

Increasing the wind parameter to $\vec{w} = 15$ resulted in a simulation that showed even more intense fire spread and selectivity (see Figure 8). As can be seen in Figure 8a, cells on the east side of the simulation burned more frequently and intensely than cells on the east side, while cells on the opposite side had an even lower rate of burning.

This trend continued as the simulation progressed (see Figures 8b and 8c, and by Figure 8d, cells on the east side had an even lower rate of burning. The total burned area also increased significantly, with a final B_F of 51.83% in Figure 8d, compared to only 3.26% in Figure 8a. It is important to note that as the wind parameter was increased, the fire spread became more complex and dynamic. The fire was no longer spreading uniformly across the simulation area, and instead, the wind direction played a significant role in determining which cells were more likely to burn.

The wind parameter was increased to 20, and the simulation showed that fire propagation was more intense than in previous iterations. The subfigures in Figure 9 depict the behavior of the fire spread when the wind parameter is set to $\vec{w} = 20$, and the direction is from west to east. As expected, the fire spread is more intense than in previous iterations, with cells burning more often and more intensely towards the wind direction. The first Figure 9a in the sequence shows a relatively low B_F rate of 2.29% at $t = 20$. However, the fire rapidly intensifies, and by $t = 40$ (Figure 9b), the B_F rate increases to 10.53%.

In Figure 9c, at $t = 60$, the B_F rate reaches 24.76%, indicating that the fire has spread to a large extent. At the end of the simulation, shown in subfigure 9d, the B_F rate is 34.86%, demonstrating the high potential of fire spread under strong wind conditions. Overall, the subfigures in Figure 9 demonstrate the importance of wind direction and speed in fire propagation. Finally, with wind $\vec{w} = 20$, the fire spreads quickly toward the lattice border, forming a triangle shape opposite to the wind direction.

4.3 Simulations considering wind direction east-west

Figure 10 shows the results of a wind simulation in the east-west direction over time, with t varying from 20 to 80. The subfigures represent the evolution of the fire in the simulation at different points in time, with the percentage of burned fuel (B_F) indicated in each subfigure.

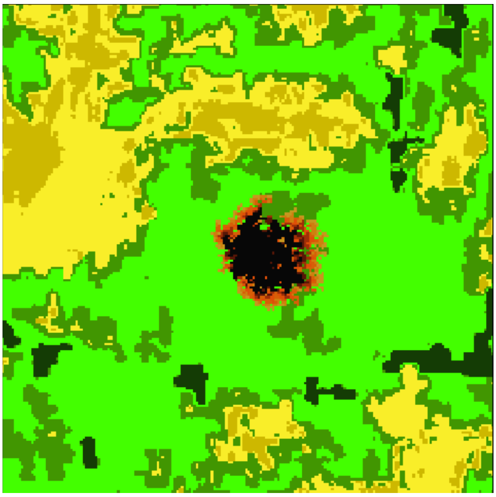

(a) $t = 20$, $B_F = 3.26\%$.

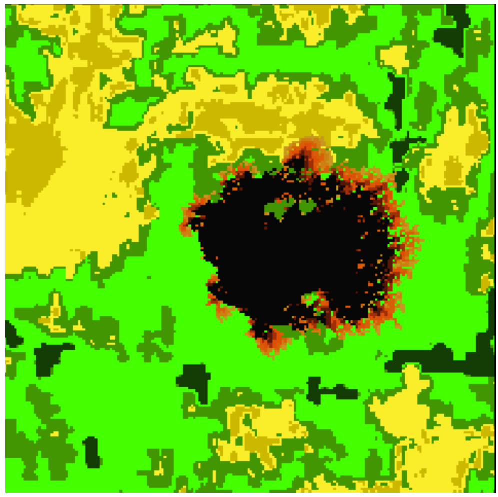

(b) $t = 40$, $B_F = 13.18\%$.

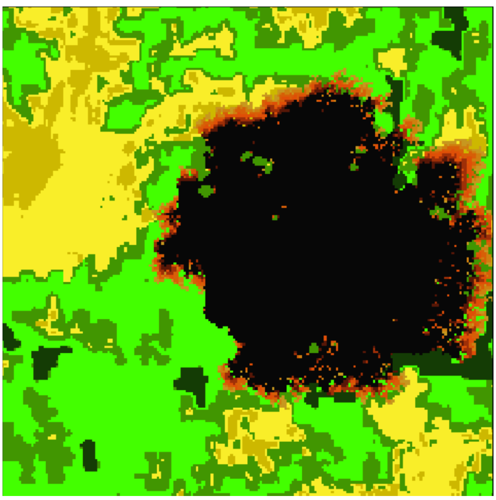

(c) $t = 60$, $B_F = 31.60\%$.

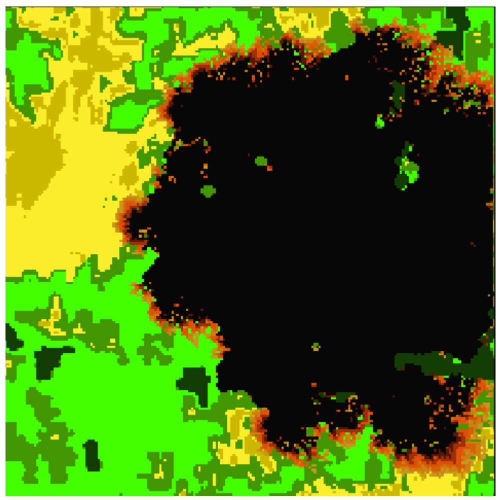

(d) $t = 80$, $B_F = 51.83\%$.

Figure 8: Experiments considering wind $\vec{w} = 15$ direction west-east.

Figure 10a shows the state of the fire at $t = 20$, with $B_F = 2.56\%$. At this point, the fire has just started and has only affected a small area.

Figure 10b shows the fire at $t = 40$, with $B_F = 11.11\%$. At this point, the fire has spread and affected a larger area. Figure 10c shows the fire at $t = 60$, with $B_F = 28.87\%$. The fire has continued to spread and has now affected a significant portion of the landscape. Finally, Figure 10d shows the fire at $t = 80$, with $B_F = 52.93\%$. At this point, the fire has reached its maximum extent and has burned over half of the fuel. Overall, the subfigures in Figure 10 demonstrate the importance of considering wind direction in fire simulations.

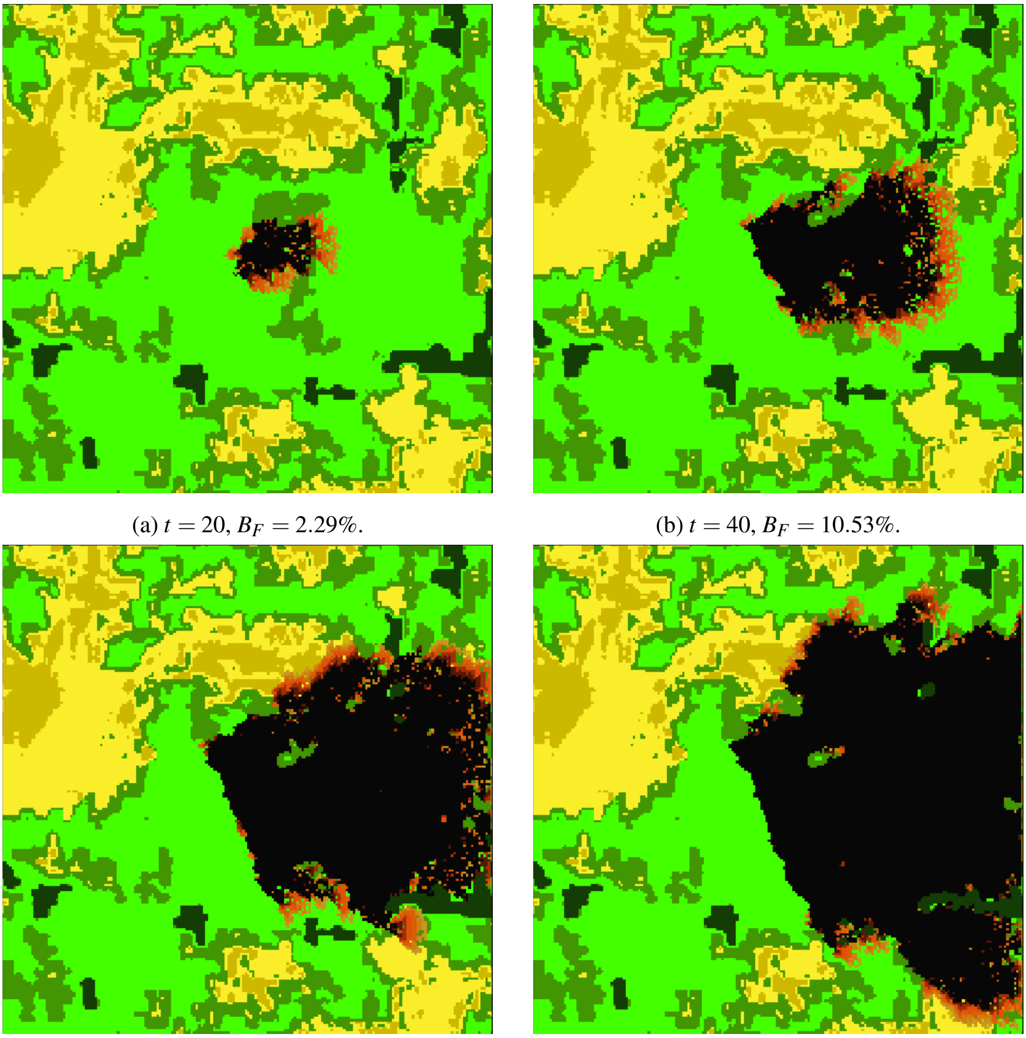

(a) $t = 20$, $B_F = 2.29\%$.

(b) $t = 40$, $B_F = 10.53\%$.

(c) $t = 60$, $B_F = 24.76\%$.

(d) $t = 80$, $B_F = 34.86\%$.

Figure 9: Experiments considering wind $\vec{w} = 20$ direction west-east.

Figure 11 presents the results of fire propagation simulations with wind blowing from east to west at different time steps (t). The Figures 11a, 11b, 11c and 11d show the burned area after the fire has propagated for a certain period of time, and the percentage of the burned area (B_F) is also provided in each subfigure.

As simulation time increases, the burned area also increases for all vegetation types. Riparian Forest and Evergreen Cerrado show lesser susceptibility, remaining largely unburned. Rupestrian Cerrado is the most susceptible, nearly completely burned, especially at the highest wind speed (Figure 11d). Figure 12 illustrates wildfire progression over time with a wind speed of $\vec{w} = 15$

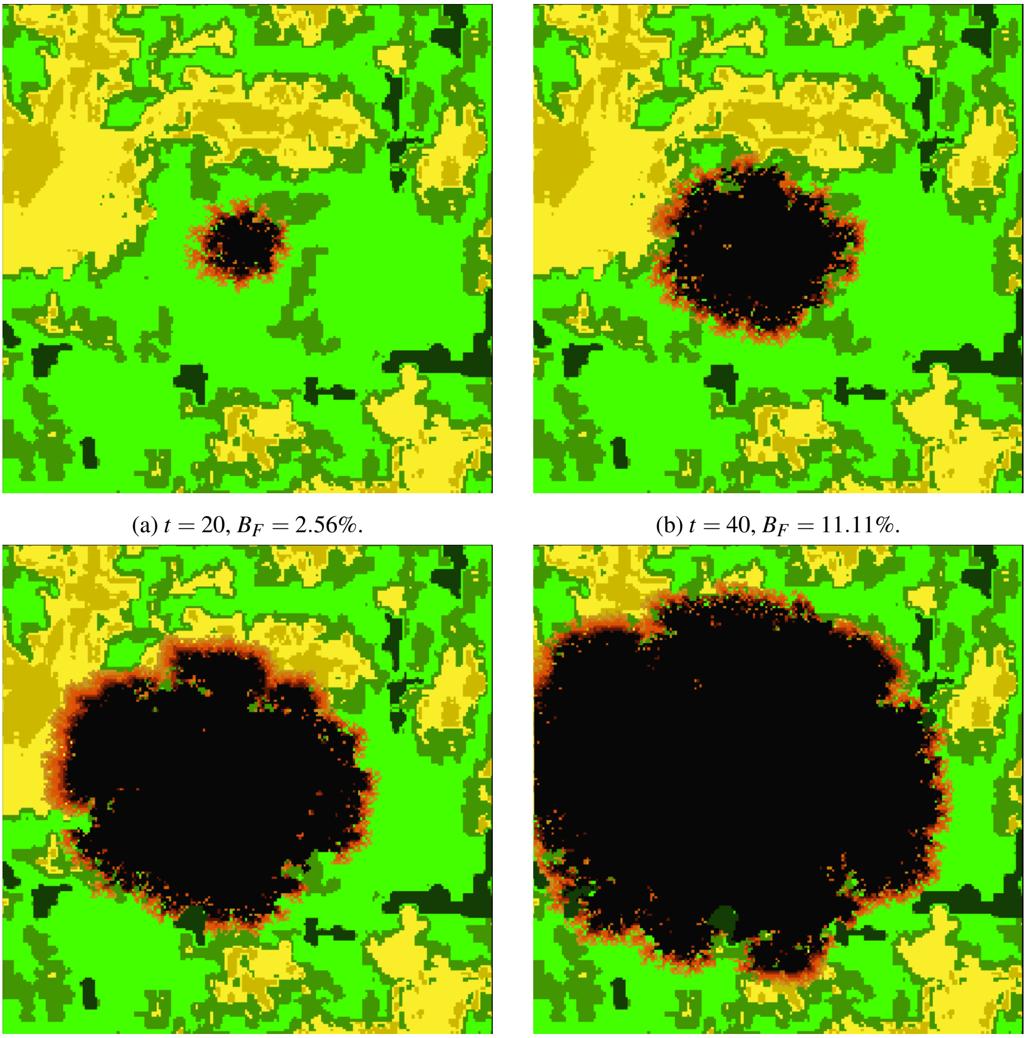

(a) $t = 20$, $B_F = 2.56\%$.

(b) $t = 40$, $B_F = 11.11\%$.

(c) $t = 60$, $B_F = 28.87\%$.

(d) $t = 80$, $B_F = 52.93\%$.

Figure 10: Experiments considering wind $\vec{w} = 5$ direction east-west.

blowing from east to west. Subfigures 12a to 12d show the spread at $t = 20$, $t = 40$, $t = 60$, and $t = 80$, with burned areas of 3.45%, 16.31%, 36.25%, and 53.97%, respectively. The images demonstrate the significant impact of wind on accelerating fire spread over successive iterations.

Figure 13 presents the results of the fire spread simulations with wind direction from east to west in the Sete Cidades National Park. The subfigures show the burned areas for different time steps (20, 40, 60, and 80) and their respective burned forest rates (B_F). The darker green areas correspond to Riparian Forest and Evergreen Cerrado, which are less susceptible to burning,

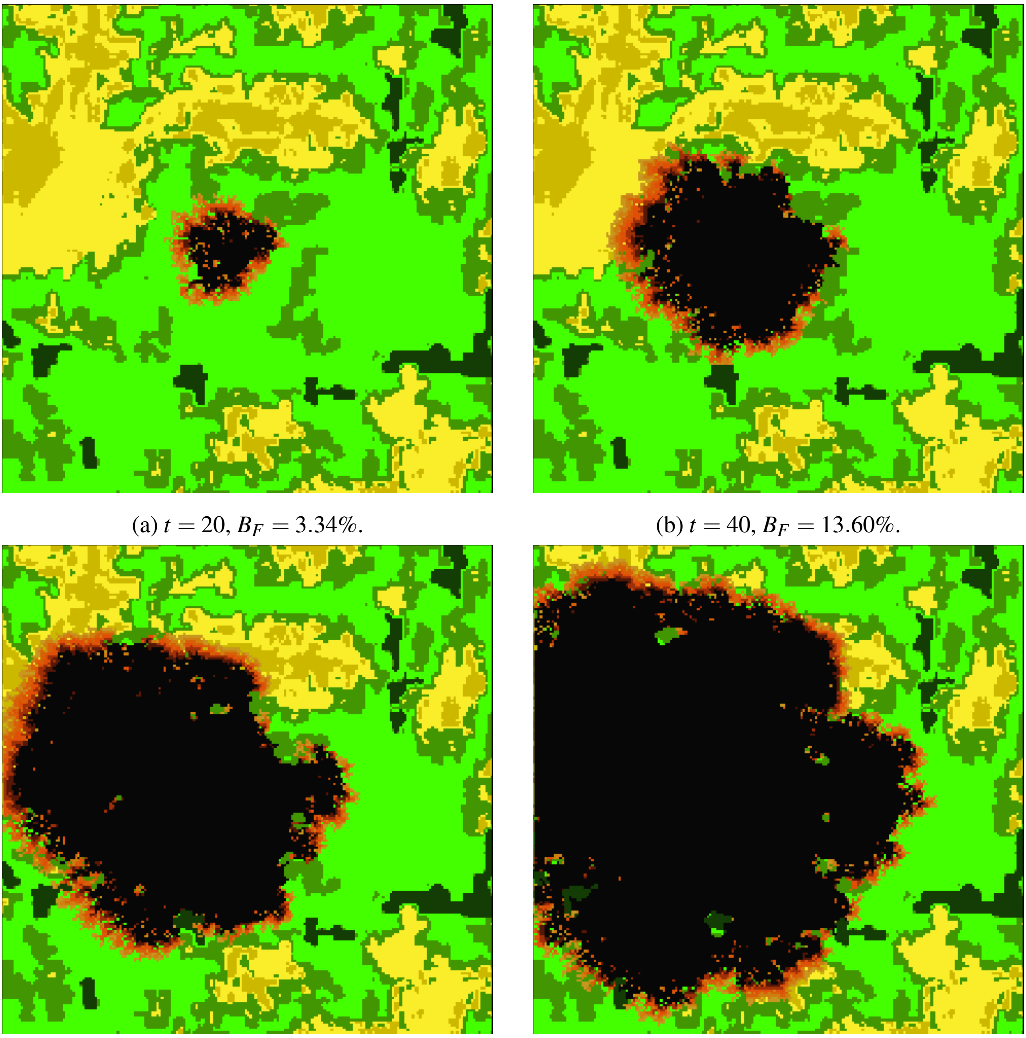

(a) $t = 20$, $B_F = 3.34\%$. (b) $t = 40$, $B_F = 13.60\%$.

(c) $t = 60$, $B_F = 32.88\%$. (d) $t = 80$, $B_F = 54.63\%$.

Figure 11: Experiments considering wind $\vec{w} = 10$ direction east-west.

followed by the green areas of Savannah Cerrado or Cerradão, which are less susceptible to burning than the yellow areas of Typical Cerrado or Rupestrian Cerrado.

Comparing the subfigures, it is possible to observe that the burned areas increase as time goes by, which is expected. Moreover, the burned forest rates also increase from 2.77% at $t = 20$ to 37.52% at $t = 80$. These results highlight the importance of early fire detection and suppression, as the longer the fire burns, the more ecosystem is impacted.

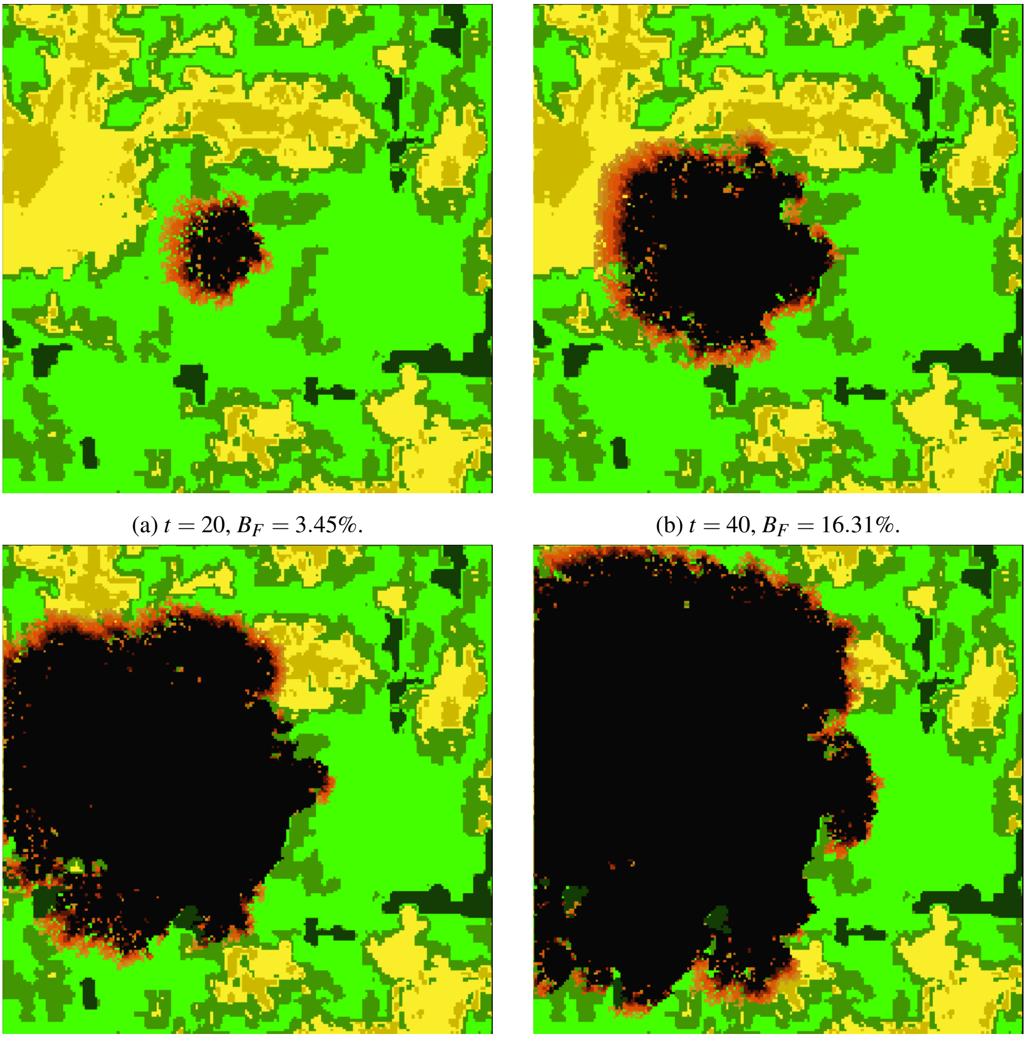

(a) $t = 20$, $B_F = 3.45\%$.

(b) $t = 40$, $B_F = 16.31\%$.

(c) $t = 60$, $B_F = 36.25\%$.

(d) $t = 80$, $B_F = 53.97\%$.

Figure 12: Experiments considering wind $\vec{w} = 15$ direction east-west.

4.4 Simulations with wind direction southeast-northwest

The figures in Figure 14 show the wind simulation in the southeast-northwest direction, with the wind speed $\vec{w} = 5$ and varying t from 20 to 80. It is possible to observe that the areas in darker green, such as the Riparian Forest and Evergreen Cerrado, are less susceptible to burning than the areas in Green (Savannah Cerrado - Cerradão), which is less susceptible to burn than vegetation in yellow (Typical Cerrado or Rupestrian Cerrado).

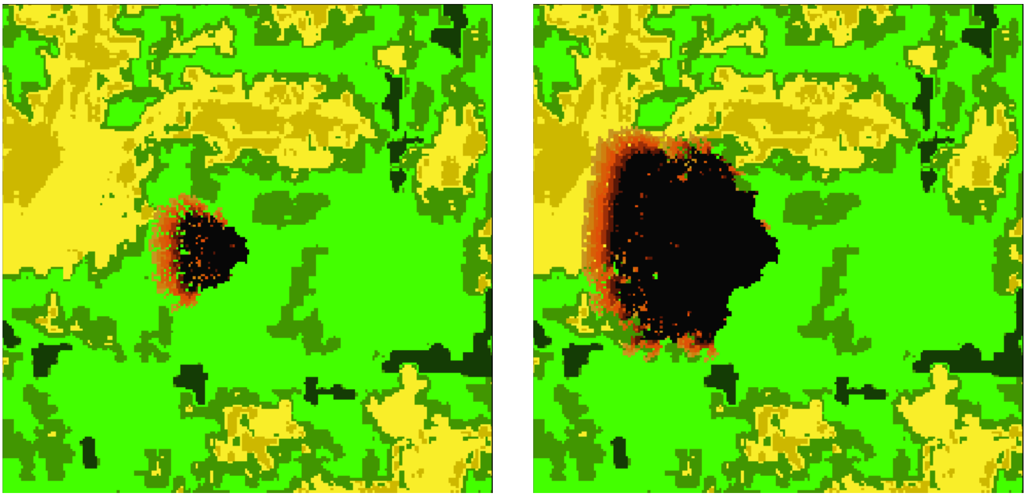

(a) $t = 20$, $B_F = 2.77\%$. (b) $t = 40$, $B_F = 12.80\%$.

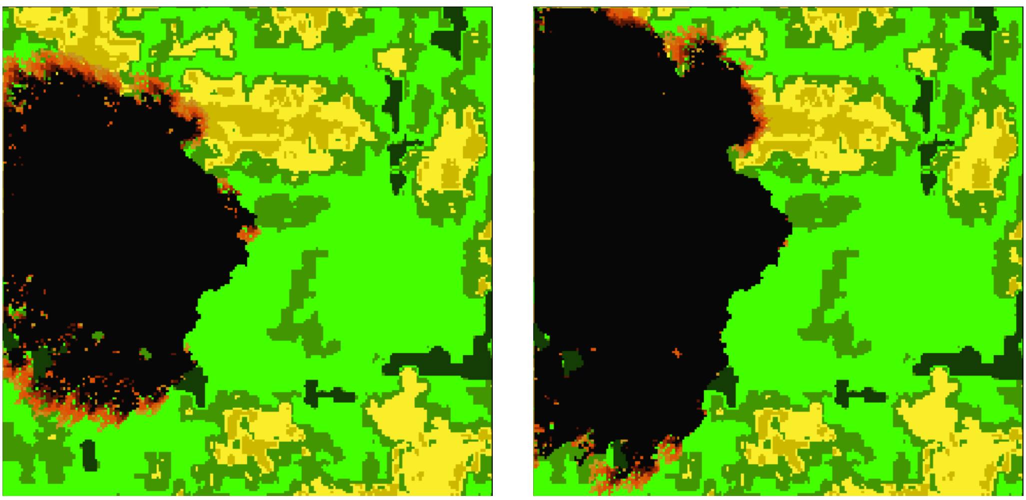

(c) $t = 60$, $B_F = 28.45\%$. (d) $t = 80$, $B_F = 37.52\%$.

Figure 13: Experiments considering wind $\vec{w} = 20$ direction east-west.

The burned forest rates B_F are presented in the captions of each subfigure. It is clear that the higher the t value, the greater the B_F rate. At $t = 20$, the B_F rate was 2.87%, which is relatively low, while at $t = 80$, it increased to 56.79%, which is very high.

The figure 15 shows the results of the simulations considering a wind with direction southeast-northwest and intensity of 10 units. The black dots represent the initial positions of the particles, and the colored dots represent their positions after a certain period of time. The color scale represents the percentage of particles that have collided with the bottom wall (floor) up to that point in time, which is known as the B_F rate. As we can see in the figure, the B_F rate increases as

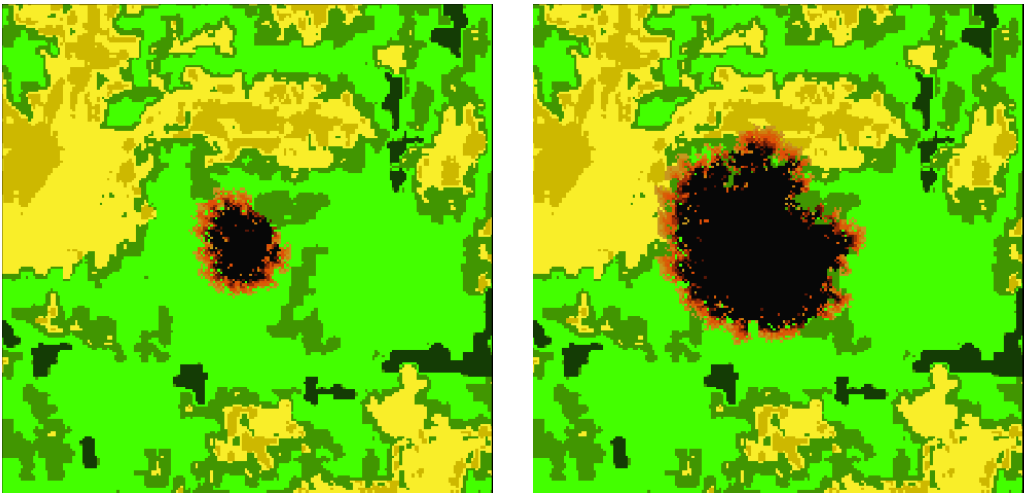

(a) $t = 20$, $B_F = 2.87\%$. (b) $t = 40$, $B_F = 11.94\%$.

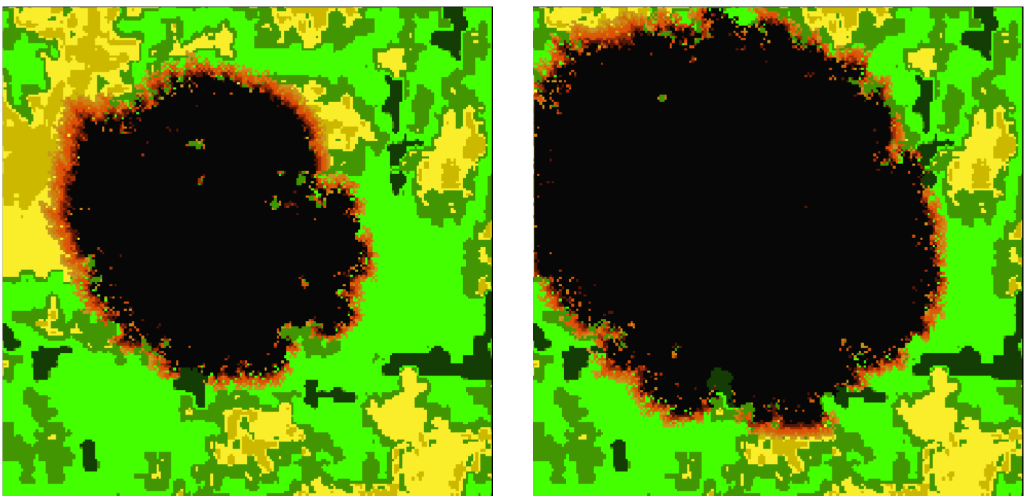

(c) $t = 60$, $B_F = 32.08\%$. (d) $t = 80$, $B_F = 56.79\%$.

Figure 14: Experiments considering wind $\vec{w} = 5$ direction southeast-northwest.

time passes and reaches 56.17% at $t = 80$. This means that more than half of the particles have already collided with the bottom wall, which indicates that the system is approaching the limit state.

This behavior can be explained by the fact that the particles at the edges of the system have more room to move and therefore take longer to reach the bottom wall. However, as time goes by, the particles become more dispersed and the probability of collision increases, which leads to a faster increase in the B_F rate.

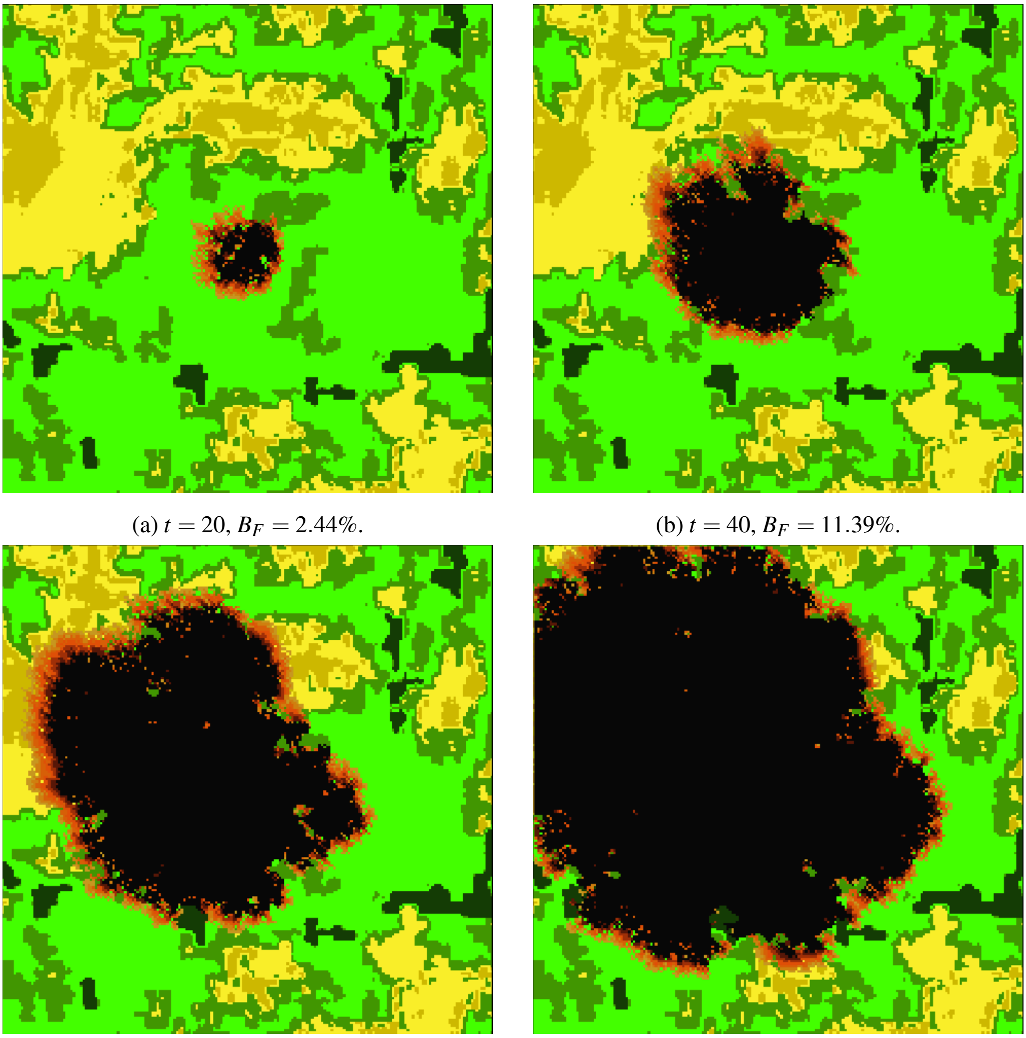

(a) $t = 20$, $B_F = 2.44\%$.

(b) $t = 40$, $B_F = 11.39\%$.

(c) $t = 60$, $B_F = 32.55\%$.

(d) $t = 80$, $B_F = 56.17\%$.

Figure 15: Experiments considering wind $\vec{w} = 10$ direction southeast-northwest.

Figure 16 shows the results of experiments where the B_F rate increases as time goes by for a fixed wind direction of $\vec{w} = 15$ in the southeast-northwest direction. From the figures, it can be observed that the density of particles increases in the direction of the wind, which is the expected behavior. Additionally, it can be seen that the higher the B_F rate, the faster the particles move in the direction of the wind. At $t = 20$, the B_F rate is 4.01%, and it can be observed in Figure 16a that the particles have moved slightly towards the northwest direction, but the density is still relatively low. As the time progresses, the B_F rate increases, and at $t = 40$ the B_F rate is 17.65%, as shown in Figure 16b. Here, it can be observed that the density of particles has increased significantly in the direction of the wind, and the particles have moved further towards the northwest direction.

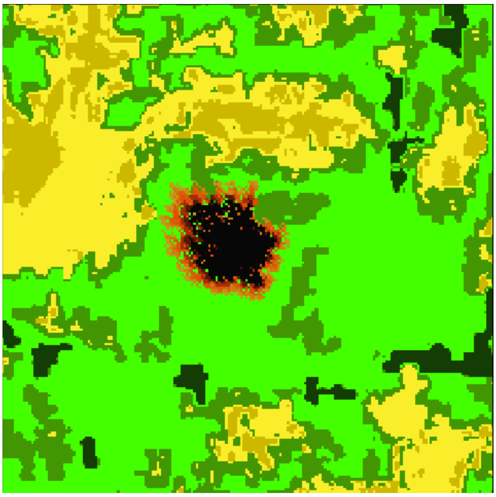

(a) $t = 20$, $B_F = 4.01\%$.

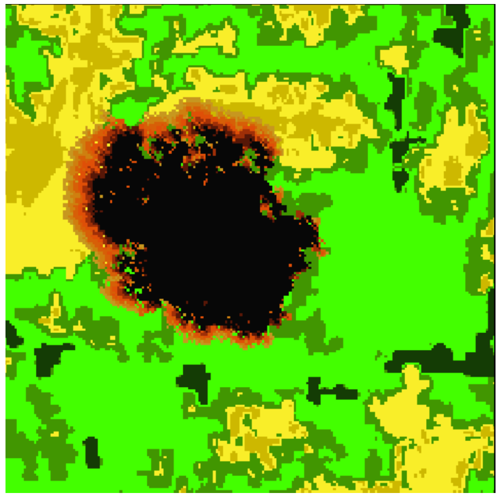

(b) $t = 40$, $B_F = 17.65\%$.

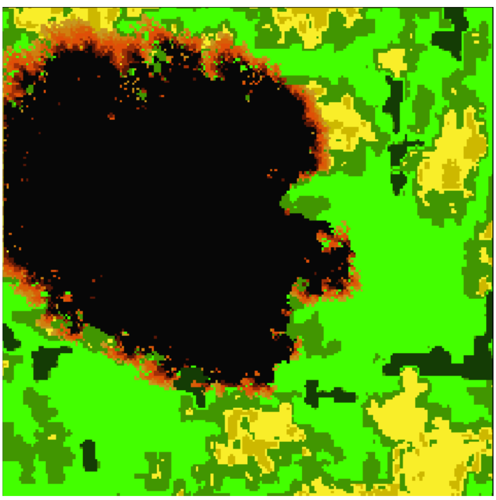

(c) $t = 60$, $B_F = 40.29\%$.

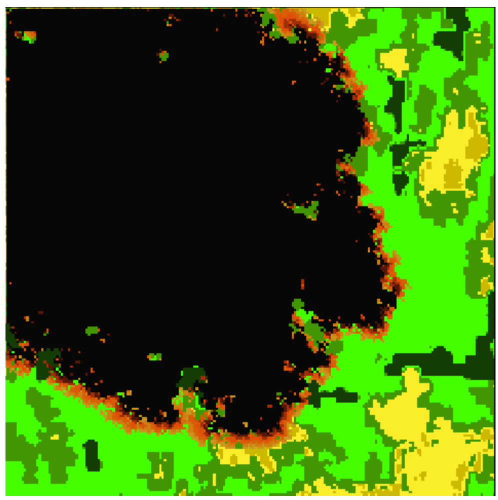

(d) $t = 80$, $B_F = 58.52\%$.

Figure 16: Experiments considering wind $\vec{w} = 15$ direction southeast-northwest.

At $t = 60$, the B_F rate is 40.29%, see Figure 16c, the density of particles in the direction of the wind is high, and the particles have moved considerably in the northwest direction. Finally, at $t = 80$, the B_F rate is 58.52%, as shown in Figure 16d, where the particles have reached the northwest boundary of the simulation domain.

The presented Figure 17 shows the results of experiments where the wind direction is southeast-northwest, and its intensity increases during time. It is possible to observe that as time goes on, the B_F rate increases, indicating a higher biomass burning area. At $t = 20$, the B_F rate is 3.18%, and the burning area is relatively small, as observed in Figure 17a. However, as time progresses, the burning area becomes more extensive, reaching 15.04% at $t = 40$, 34.07% at $t = 60$, and 46.32% at $t = 80$ (Figures 17b, 17c, and 17d, respectively).

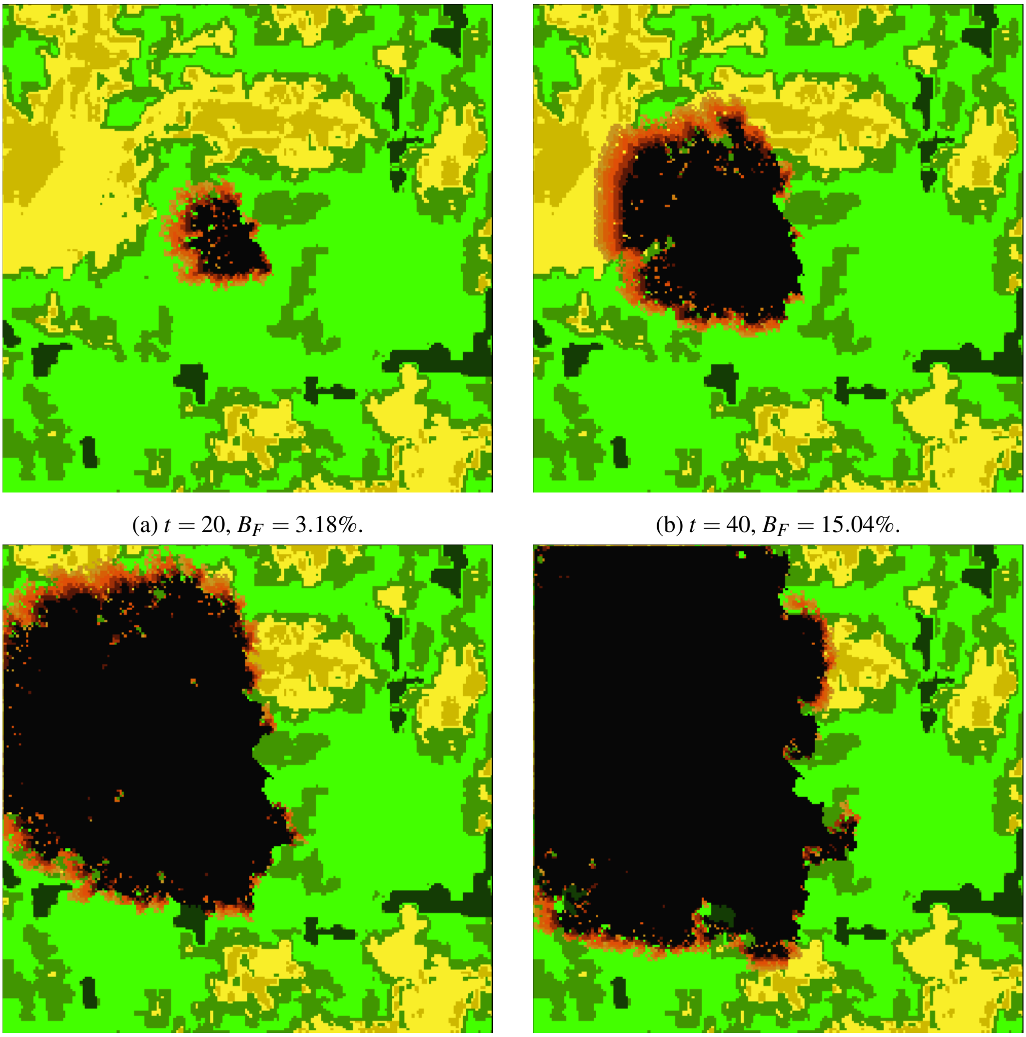

(a) $t = 20$, $B_F = 3.18\%$.

(b) $t = 40$, $B_F = 15.04\%$.

(c) $t = 60$, $B_F = 34.07\%$.

(d) $t = 80$, $B_F = 46.32\%$.

Figure 17: Experiments considering wind $\vec{w} = 20$ direction southeast-northwest.

This behavior can be explained by the fact that as the wind intensity increases, it carries the fire to new areas, causing the burning area to expand. Additionally, the higher the wind intensity, the more oxygen is supplied to the fire, causing it to burn more intensely.

5 CONCLUSIONS AND FUTURE WORK

In conclusion, the experiments conducted in Sete Cidades National Park provide valuable information about the impact of wind speed and direction on fire propagation in different vegetation types. The results highlight the importance of considering these factors when developing prevention and control strategies for wildfires. The experiments show that increasing wind speed leads to more extensive burning, with the fire spread intensifying and becoming even more selective. Vegetation type also plays a crucial role in fire susceptibility, with some areas being less vulnerable to burning than others. The results suggest that early detection and control measures are crucial to minimize the impact of wildfires.

Although the experiments provide valuable insights, they also have some limitations. The simulations are based on a model that may not fully capture the complexity of real-world wildfire dynamics. The experiments are also limited to specific wind directions and speeds and vegetation types, and may not be fully representative of other regions or ecosystems. Future work could include expanding the experiments to other regions and ecosystems to further validate the results. Additionally, the experiments could be refined to incorporate additional factors that may influence wildfire behavior, such as topography, humidity, fuel availability and also includes Potts Markov random field model to compute the probabilities of vegetation getting fire. These improvements could lead to more accurate fire spread models and better-informed fire management strategies, ultimately helping to minimize the impact of wildfires on natural ecosystems and human settlements.

REFERENCES

[1] S.T. Alvarado, I.S. de Carvalho, T.M. Ferraz & T.S. Silva. Effects of fire suppression policies on fire regimes in protected areas in the Cerrado. *Biodiversidade Brasileira-BioBrasil*, **1** (2019), 200–200.

[2] H.C. Brasiel & D.A. Lima. Exploring the influence of wind, vegetation and water sources on the spread of forest fires in the Brazilian Cerrado Biome using Cellular Automata. In “Anais do XIV Workshop de Computação Aplicada à Gestão do Meio Ambiente e Recursos Naturais”. SBC (2023), p. 61–70.

[3] S. Darmawan, D.K. Sari, K. Wikantika, A. Tridawati, R. Hernawati & M.K. Sedu. Identification before-after forest fire and prediction of mangrove forest based on Markov-cellular automata in part of Sembilang national park, Banyuasin, South Sumatra, Indonesia. *Remote Sensing*, **12**(22) (2020), 3700.

[4] M. El Naschie. Cellular automata based on the golden mean number system as a foundation for artificial intelligence and artificial life. *International Journal of Artificial Intelligence and Mechatronics*, **8**(6) (2020).

[5] S. Fabbri, C. Silva, E. Hernandes, F. Octaviano, A. Di Thommazo & A. Belgamo. Improvements in the StArt tool to better support the systematic review process. In “Proceedings of the 20th international conference on evaluation and assessment in software engineering” (2016), p. 1–5.

[6] M.E.A. Ferreira, A.L. Quinta, D.A. Lima, L.G. Martins & G. Oliveira. Automatic Evolutionary Adjustment of Cellular Automata Model for Forest Fire Propagation. In “International Conference on Cellular Automata for Research and Industry”. Springer (2022), p. 235–245.

[7] N.M. Gharakhanlou & N. Hooshangi. Dynamic simulation of fire propagation in forests and rangelands using a GIS-based cellular automata model. *International Journal of Wildland Fire*, **30**(9) (2021), 652–663.

[8] F. Giannino, L. Russo, D. Ascoli, A. Migliozzi, C.I. Siettos & S. Mazzoleni. Cellular automata simulation of forest fire behavior on Italian landscape: The case of Sardinia. In “AIP Conference Proceedings”, volume 1906. AIP Publishing LLC (2017), p. 100006.

[9] S. Hesam & K.V. Kamran. Intelligent management occurrence and spread of front fire in gis by using cellular automata. Case study: Golestan forest. *International Archives of the Photogrammetry, Remote Sensing & Spatial Information Sciences*, (2019).

[10] K. Horibe, K. Walker & S. Risi. Regenerating soft robots through neural cellular automata. In “Genetic Programming: 24th European Conference, EuroGP 2021, Held as Part of EvoStar 2021, Virtual Event, April 7–9, 2021, Proceedings 24”. Springer (2021), p. 36–50.

[11] B. Kitchenham, O.P. Brereton, D. Budgen, M. Turner, J. Bailey & S. Linkman. Systematic literature reviews in software engineering–a systematic literature review. *Information and software technology*, **51**(1) (2009), 7–15.

[12] D.A. Lima, E. Cabral Jr, I.T. Almeida, J.P. Andrade, J.P. Fonseca, M.E. Santos, N.T. Nunes & V.H. Bernardes. A fire elitist cellular automaton-based model to verify pedestrian flow simulated in real environments using Arduino. *Proc. Series of the Brazilian Society of Computational and App. Mathematics*, **7**(1) (2020).

[13] H.A. Lima & D.A. Lima. Autômatos celulares estocásticos bidimensionais aplicados a simulação de propagação de incêndios em florestas homogêneas. In “Workshop de Computação Aplicada a Gestão do Meio Ambiente e Recursos Naturais”. SBC (2014), p. 15–24.

[14] E.R. Lira, H.B. de Macêdo, D.A. Lima, L. Alt & G. Oliveira. A reversible system based on hybrid toggle radius-4 cellular automata and its application as a block cipher. *Natural Computing*, (2023), 1–17.

[15] H.J. Lopes & D.A. Lima. Cellular Automata in path planning navigation control applied in surveillance task using the e-Puck architecture. In “2020 IEEE International Conference on Systems, Man, and Cybernetics (SMC)”. IEEE (2020), p. 1117–1122.

[16] M.d.Q. Matos & J.M. Felfili. Florística, fitossociologia e diversidade da vegetação arbórea nas matas de galeria do Parque Nacional de Sete Cidades (PNSC), Piauí, Brasil. *Acta botânica brasílica*, **24** (2010), 483–496.

[17] M.E.A. Oliveira, F.R. Martins, A. Castro & J.R.d. Santos. Classes de cobertura vegetal do Parque Nacional de Sete Cidades (transição campo-floresta) utilizando imagens TM/Landsat, NE do Brasil. *XIII Simpósio Brasileiro de Sensoriamento Remoto*, **13** (2007).

[18] A. Schadschneider, A. Kirchner & K. Nishinari. CA approach to collective phenomena in pedestrian dynamics. In "Cellular Automata: 5th International Conference on Cellular Automata for Research and Industry, ACRI 2002 Geneva, Switzerland, October 9–11, 2002 Proceedings 5". Springer (2002), p. 239–248.

[19] D.H. Serrano & A.M. del Rey. Virtual cyclic cellular automata, finite group actions and recursive properties. *Information Sciences*, **608** (2022), 917–930.

[20] A.W. Setzer, R.A. Sismanoglu & J.G.M.d. Santos. Metodo do Calculo do Risco de Fogo do Programa do INPE - Versao 11, Junho/2019. In "Relatorio Tecnico do Instituto Nacional de Pesquisas Espaciais". INPE (2019), p. 1–29. URL `sid.inpe.br/mtc-m21c/2019/11.21.11.03-PRP`.

[21] W. Sun, W. Wei, J. Chen & K. Ren. Research on Amazon Forest Fire Based on Cellular Automata Simulation. In "2021 20th International Symposium on Distributed Computing and Applications for Business Engineering and Science (DCABES)". IEEE (2021), p. 175–178.

[22] C. Tavares & M. Lazo. Dynamic Systems with Fractional Derivatives Applied to Interagent Populations Problems. *Trends in Computational and Applied Mathematics*, **23** (2022), 299–314.

[23] S. Wolfram & M. Gad-el Hak. A new kind of science. *Appl. Mech. Rev.*, **56**(2) (2003), B18–B19.

[24] J. Zeng, Y. Qian, P. Mi, C. Zhang, F. Yin, L. Zhu & D. Xu. Freeway traffic flow cellular automata model based on mean velocity feedback. *Physica A: Statistical Mechanics and its Applications*, **562** (2021), 125387.

[25] Y. Zhang & J. Zhang. Modeling of solidification microstructure evolution in laser powder bed fusion fabricated 316L stainless steel using combined computational fluid dynamics and cellular automata. *Additive Manufacturing*, **28** (2019), 750–765.

How to cite

Brasiel H.C. & Lima D.A. Enhancing wildfire simulation with wind and vegetation parameters using Cellular Automata in Sete Cidades National Park: a study in the Brazilian Cerrado biome. *Trends in Computational and Applied Mathematics*, **25**(2024), e01757. doi: 10.5540/tcam.2024.025.e01757.